Investigation of the Two-Step Spin Crossover Complex Fe[5-NO_2-sal-(1,4,7,10)] Using Density Functional Theory

Thomas Guillon,[†] Lionel Salmon,[†] Gábor Molnár,[†] Samir Zein,[‡] Serguei Borshch,[‡] and Azzedine Bousseksou*,[†]

Laboratoire de Chimie de Coordination, UPR 8241 CNRS, 205 route de Narbonne, 31077 Toulouse Cedex, France, and Laboratoire de Chimie, UMR 5182 CNRS, Ecole Normale Supérieure de Lyon, 46 allée d'Italie, 69364 Lyon Cedex 07, France

Received: March 1, 2007; In Final Form: April 26, 2007

A quantum chemical study of the Fe[5-NO_2-sal-(1,4,7,10)] ((1,10-bis(5-nitrosalicylaldehyde)-1,4,7,10-tetraezdecane-*O*,*O*′,*N*,*N*′,*N*″,*N*‴)iron(II)) molecule was performed using density functional theory (DFT). Starting from the different X-ray crystallographic structures, geometry optimizations have been performed. These calculations confirmed the conformational isomerism of this complex in each spin states of the molecule ($^1A_{1g}$ and $^5T_{2g}$). Each employed DFT method (B3LYP, B3LYP*, BP86, HCTH407) reproduced correctly the structural differences between the two calculated conformers when compared to the experimental structures. Furthermore, electronic polarizabilities have been calculated in each spin state and for each conformer. These calculations revealed a higher polarizability in the singlet state in agreement with the measured higher dielectric constant in this state.

Introduction

Certain $3d^4-3d^7$ transition metal complexes are known to display a molecular bistability between high-spin (HS) and low-spin (LS) electron configurations, which are distinguished by different occupation of antibonding e_g and nonbonding t_{2g} 3d orbitals of the central metal ion.[1,2] The electronic ground state of these spin crossover (SCO) complexes may be reversibly interchanged under external stimuli, such as temperature, pressure, magnetic field, or light irradiation. The molecular structure of these complexes is significantly different in the two spin states. In particular, the metal−ligand bond lengths of the HS compounds with occupied antibonding e_g orbitals are substantially larger than those of LS compounds. The difference between the two metal−ligand bond lengths is typically around 0.2 Å in complexes with $Fe(II)N_6$ coordination core, which corresponds to a change of ca. 10%. This bond length change is accompanied also by the change of bond angles.[2]

A few SCO compounds like $[Fe(phen)_2(NCS)_2]$ (phen = 1,-10 phenantroline) and $[Fe(PM\text{-}BiA)_2(NCS)_2]$ (PM-BiA = *N*-(2-pyridylmethylene)-4-aminobiphenyl) are constituted by two enantiomers (Λ and Δ) per unit cell whatever the value of the temperature, i.e., in both the LS and HS states. The Fe[5-NO_2-sal-(1,4,7,10)] complex ((1,10-bis(5-nitrosalicylaldehyde)-1,4,7,-10-tetra-ezdecane-*O*,*O*′,*N*,*N*′,*N*″,*N*‴)iron(II)) is constituted by two Λ and Δ molecules per unit cell, which are enantiomers at room temperature, but the two molecules are differently deformed upon cooling.[3,4] This compound presents a singular behavior in that its magnetic moment displays a double-step thermal spin crossover phenomenon with two transitions separated by a plateau of ca. 30 K (Figure 1). This plateau corresponds to 50% spin state change. The two transitions occur with hysteresis: in the heating mode they occur at around 145 and 177 K, and in the cooling mode they occur at around 173 and 136 K.

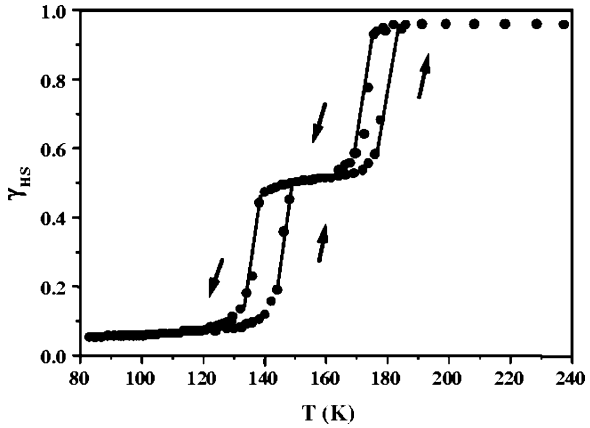

Figure 1. Thermal variation of the proportion of high-spin molecules (γ_{HS}) in Fe[5-NO_2-sal-N(1,4,7,10)] obtained through magnetic susceptibility measurements.[3,4] (Data points are connected to guide the eye.)

Thermal spin crossover phenomenon is known to occur either gradually or abruptly with or without a hysteresis loop. In a few complexes the temperature dependence of the high-spin fraction displays atypical two-step behavior,[3−7] which has received much attention from the theoretical point of view.[4,8−12] Two-step curves can be obtained trivially by considering two crystallographically different metal ions, but two-step behavior can also be predicted for structurally equivalent sublattices[6,10] or binuclear molecules[12] if the model combines negative and positive interactions (long and short range, respectively). The two-step behavior in the case of the title complex is unique because it is accompanied also by two hysteresis loops. The origin of the two-step behavior in this complex was explained thanks to comparative crystallographic studies on the [Fe(3X,-4Y,5Z-sal-N(1,4,7,10))] family.[13] The crystalline lattice packing

[†] Laboratoire de Chimie de Coordination, UPR 8241 CNRS.
[‡] Laboratoire de Chimie, UMR 5182 CNRS.

10.1021/jp071686l CCC: $37.00
Published on Web 06/14/2007

corresponds to a one-dimensional (1D) chain in which an alternation of Λ and Δ molecules in the cis α conformation is observed. Along these chains, the "strong" hydrogen bonds between the molecules explain the cooperativity of the system and the first-order spin transition. Moreover, the parallel arrangement of the 1D chains leads to an important structural anisotropy. As a consequence, a two-step spin crossover accompanied by two structural phase changes occurs (*P*2/*c* at 295 K, *P*2 at 153 K, and *P*1 at 102 K). An important finding is that the molecules are very close to each other and the occupied volume by each molecule is especially small. Therefore the change of the spin state of one molecule (for example Λ) induces a ligand field change on its neighbor (Δ), preventing its spin state change in the same temperature ("short-range, negative interaction"[8,10]).

In this paper we report DFT calculations on the Fe[5-NO_2-sal-(1,4,7,10)] complex in the different spin states. The aim of this study was to investigate theoretically the conformational isomerism of this complex in the two spin states in order to confirm and better understand the experimental findings,[4] which have been debated in the literature.[13] Furthermore, we wished to test the potential of DFT calculations for predicting geometries and energies of such large transition metal complexes displaying spin state as well as conformational changes. On the other hand, this compound displays also a rather curious dielectric behavior. Several reports have shown that the dielectric constant of SCO complexes is significantly higher in the HS state when compared to the LS state.[14] However, in the case of the Fe[5-NO_2-sal-(1,4,7,10)] complex the opposite situation has been observed.[14] To try to explain this result, we have calculated also the dependence of the microscopic electrical properties on the spin state through the evaluation of the electronic polarizability of the molecule in the two spin states.

Methods

Density functional theory calculations were performed with the Gaussian 03 program package.[15] Becke's three-parameter hybrid functional B3LYP[16] and the reparametrised B3LYP* [17] were used with several basis sets: 6-31G*, 6-311+G**, TZVP,[18] LANL2DZ.[19] Calculations were also performed with the BP86 and HCTH407 GGA functional methods using the TZVP basis set. The X-ray crystallographic structure data were used as the starting point for the optimizations of the geometries.[4] X-ray crystallographic structures at 153 and 293 K are given in the literature without hydrogen atoms and in these cases we used the software MaterialStudio[20] and the software packages Cerius2[21] with InsightII[22] for adding hydrogen on their carrier atoms. First, geometry optimizations were performed for the added H atoms, freezing all other atoms. Then, total geometry optimizations were performed. The MOLDEN[23] and the MOLEKEL[24] software packages were used to visualize the calculated molecular structures. After completing the optimization, vibrational frequencies (within the harmonic approximation) and the static polarizability tensor were calculated.

Results and Discussion

Structures. The large number of atoms in the SCO complexes does not permit the use of computationally demanding high-level ab initio (i.e., wavefunction-based) methods, but DFT methods can be applied to such large systems. DFT calculations have recently been carried out on several SCO compounds.[12,25−30] These studies were aimed at assessing the performance of available density functional methods for describing the geometries of the complexes in both spin states, for evaluating the HS-LS energy difference and to determine the vibrational spectra. While the absolute values of HS-LS energy differences were often inaccurately determined, it was shown that DFT methods are able to reproduce a correct behavior of the energy gap in series of similar spin transition complexes and give structural parameters in good agreement with the experimental data.

DFT calculations have been performed on the complex Fe[5-NO_2-sal-(1,4,7,10)] starting from the different X-ray crystallographic structures obtained at three temperatures (102, 153, and 295 K) by Boinnard et al.[4] According to the crystallographic data, this complex presents two (Λ and Δ) enantiomers at room temperature. At 153 K, i.e., in the plateau region, the LS Λ molecules are slightly deformed in comparison with the Δ molecules that retain the HS state. The deformation of the former molecule corresponds mainly to the contraction of the coordination sphere of the iron, typically observed during the HS → LS spin crossover phenomenon. At low temperature (102 K) both molecules are in the LS state, but the Δ molecules are much more deformed than the Λ molecules and correspond clearly to another conformer.

Total geometry optimizations were performed starting from each available experimental structure in both spin multiplicities without symmetry constraints. Remarkably, two different optimized structures, corresponding to two minima on the potential energy surface (a local minimum and a global one), were obtained in both spin states (Figure 2). This result is general in that it was found independently of the calculation method. The two optimized structures, which are conformational isomers, are named "structure a" and "structure b". Geometry optimization procedures using the 295 and 153 K experimental structures as well as the "102 K−Λ" structure converged always to the same structure a. On the other hand, when the input was the 102 K−Δ structure the geometry optimization converged to the structure b—either in the HS or in the LS state. We must notice that HS state structure b has not been observed experimentally. Furthermore, in contrast to the experimental situation, the optimized structures display necessarily eniantiomerism for both structure a and structure b (named Λa, Δa, Λb, and Δb) and in each spin state.

Table 1 provides a comparison between X-ray crystallographic data and calculated metal−ligand bond distances of the complex Fe[5-NO_2-sal-(1,4,7,10)] in both spin states. Calculated values of bond distances reproduce the measured ones with correct accuracy with hybrid functional and GGA functional methods. The metal−ligand bond distances are known to be deeply affected by the spin state change. Indeed, the mean Fe−N bonds length increases from 2.02 Å (2.00 Å) to 2.24 Å (2.24 Å) for structure a (structure b) when going from the LS to the HS state, which compares well with the experimental data where a change from 2.06 Å (2.01 Å) to 2.18 Å has been observed (Table 1, see also Supporting Information). In general B3LYP, B3LYP*, BP86, and HTCH407 methods give good Fe−N bond length values and, as expected, HF methods largely overestimate them. This tendency was observed earlier for many spin crossover complexes.[12,25−30] HF methods slightly overestimate Fe−O bonds length values whereas all other methods slightly underestimate them. The Fe−O bonds in the HS state are approximately 0.07 Å longer when compared to the LS state in the calculations but remain approximately constant within the experimental errors. Bond angle and dihedral angle values are also in reasonable agreement between experimental and calculation for each method (Tables 2 and 3, see also Supporting

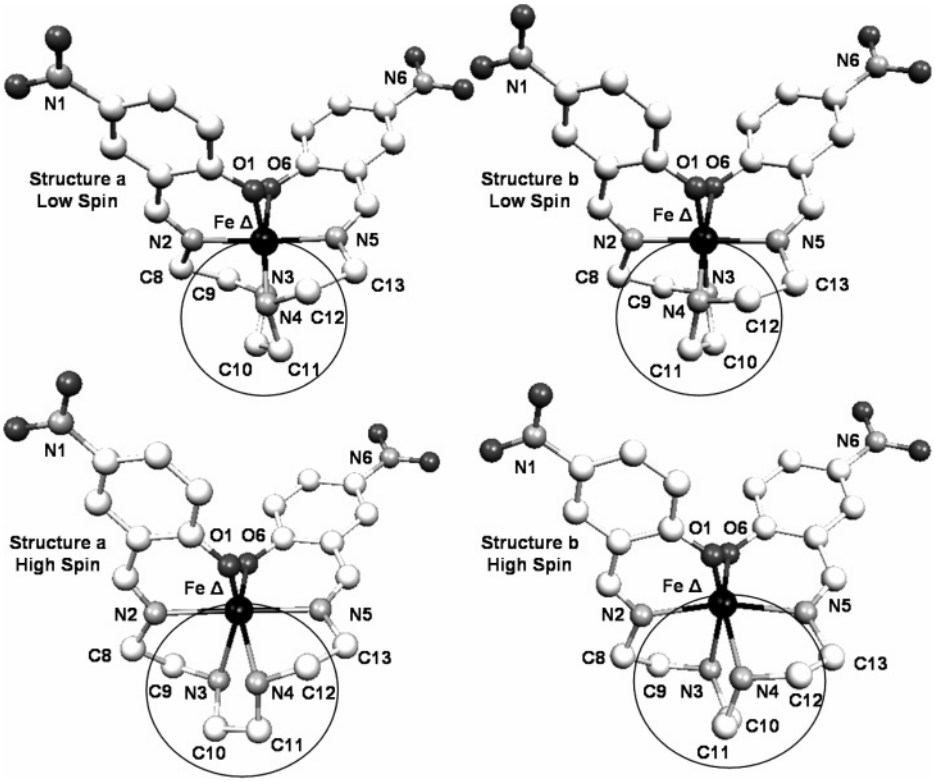

Figure 2. Optimized structures (B3LYP/TZVP) in the LS and HS states on the example of the Δ enantiomorph.

TABLE 1: Experimental[4] and Calculated (B3LYP*/TZVP) Fe−Ligand Bond Lengths (Å)[a]

	X-ray (103 K) structure a	LS structure a	X-ray (103 K) structure b	LS structure b	X-ray (292 K) structure a	HS structure a	HS structure b
$Fe-N_2$	2.20(2)	1.966	1.75(3)	1.953	2.127(4)	2.157	2.166
$Fe-N_5$	1.83(3)	1.966	2.14(3)	1.953	2.127(4)	2.184	2.166
$Fe-N_3$	2.08(4)	2.070	2.11(4)	2.048	2.235(4)	2.317	2.314
$Fe-N_4$	2.13(4)	2.070	2.06(4)	2.048	2.235(4)	2.320	2.314
$Fe-O_1$	2.07(3)	1.971	1.84(3)	1.965	2.041(4)	2.007	2.027
$Fe-O_6$	2.03(3)	1.971	1.96(3)	1.965	2.041(4)	2.073	2.028

[a] Note: HS "structure b" has not been observed experimentally.

TABLE 2: Experimental[4] and Calculated (B3LYP*/TZVP) Fe−Ligand Bond Angles[a]

	X-ray (103 K) structure a	LS structure a	X-ray (103 K) structure b	LS structure b	X-ray (292 K) structure a	HS structure a	HS structure b
O_1-Fe-N_2	85(1)	92.0	100(1)	92.1	86.0(2)	85.5	84.9
O_1-Fe-N_3	160(1)	172.2	174(1)	175.4	159.1(2)	157.2	159.3
O_1-Fe-O_6	99(1)	93.3	91(1)	92.2	98.5(2)	108.3	102.0
O_1-Fe-N_5	99(1)	85.3	80(1)	88.1	93.4(2)	96.5	104.0
O_1-Fe-N_4	97(1)	91.6	91(1)	90.9	95.2(2)	95.3	92.7
N_2-Fe-O_6	90(1)	85.3	95(1)	88.1	93.4(2)	95.1	104.0
N_2-Fe-N_5	175(1)	176.0	179(2)	179.8	179.1(2)	178.0	165.9
N_2-Fe-N_3	76(1)	82.3	80(2)	84.6	77.4(2)	76.6	77.2
N_2-Fe-N_4	103(1)	100.7	91(2)	95.2	103.3(2)	104.4	91.8
N_3-Fe-O_6	89(2)	91.6	96(2)	90.9	95.2(2)	87.5	92.5
N_3-Fe-N_5	100(1)	100.7	100(1)	95.2	103.3(2)	101.5	91.7
N_3-Fe-N_4	80(2)	84.2	83(2)	86.1	76.7(2)	76.0	77.6
O_6-Fe-N_5	93(1)	92.0	86(1)	92.1	86.0(2)	84.2	84.9
O_6-Fe-N_4	160(1)	172.2	173(1)	175.4	159.1(2)	150.5	159.1
N_4-Fe-N_5	74(1)	82.3	88(1)	84.6	77.4(2)	75.6	77.2

[a] Note: HS "structure b" has not been observed experimentally.

Information) especially as far as the changes between the conformers are concerned.

The global geometry of the optimized LS structure a is fairly similar to the HS structure a and the same is true also for the HS and LS structure b (even though the Fe−ligand bond lengths are different in the two spin states). The optimized Fe−ligand bond lengths in LS state are slightly smaller in structure b when compared to the other conformer in agreement with the

TABLE 3: Experimental[4] and Calculated (B3LYP*/TZVP) Dihedral Angles around the Central Atom Group −N3−C10−C11−N4− (Circle in Figure 2)[a]

	X-ray (103 K) structure a	LS structure a	X-ray (103 K) structure b	LS structure b	X-ray (292 K) structure a	HS structure a	HS structure b
$N_4-C_{11}-C_{10}-N_3$	+70.9	+48.0	−29.9	−40.1	+53.8	+55.5	−44.4
$Fe-N_4-C_{11}-C_{10}$	−51.8	−35.7	+21.4	+29.7	−40.4	−40.1	+32.2
$Fe-N_3-C_{10}-C_{11}$	−54.1	−35.7	+23.9	+29.7	−40.4	−41.3	+32.2
$C_{12}-N_4-C_{11}-C_{10}$	−173.5	−151.9	−95.1	−91.1	−159.5	−158.3	−90.3
$C_9-N_3-C_{10}-C_{11}$	−170.8	−151.9	−105.3	−91.1	−159.5	−158.9	−90.3
$N_4-C_{12}-C_{13}-N_5$	+37.4	+40.5	+24.8	+43.0	+45.2	+44.9	+46.5
$N_3-C_9-C_8-N_2$	+58.8	+40.5	+42.3	+43.0	+45.2	+46.4	+46.5
$O_1-Fe-N_4-C_{11}$	+178.4	+173.9	+174.2	+165.8	+174.7	+172.3	+150.2
$O_6-Fe-N_3-C_{10}$	−174.5	+173.9	+161.7	+165.8	+174.7	+170.4	+150.1
$N_5-Fe-N_4-C_{11}$	−91.8	−88.9	−106.4	−106.3	−93.0	−92.3	−106.0
$N_2-Fe-N_3-C_{10}$	−77.5	−88.9	−103.8	−106.3	−93.0	−93.8	−106.1

[a] Note: Values are given in the case of Δ molecules for more clarity (values for Λ molecules have opposite signs). HS "structure b" has not been observed experimentally.

experimental data. On the other hand, the difference between the two HS conformers remains relatively small. The main structural difference between the two conformational isomers consists of a rearrangement of the tetraamine chain with a clear distortion of the central atom group −N3−C10−C11−N4− (circle in Figure 2). Selected values of the measured and calculated dihedral angles of the tetraamine chain are reported in Table 3. (See also Supporting Information.) In particular, we can notice the calculated difference of the dihedral angle values −N3−C10−C11−N4− between the two conformers, equals to approximately 90° in both spin states in good agreement with the experimental findings. The other calculated dihedral angles, reported in Table 3 reproduce also satisfactorily the changes observed in the experiments.

With each DFT method, the two optimized geometries in the LS and HS states present a C_2 and C_1 symmetry, respectively. The symmetry of the optimized structure a in HS state is lower than this of the optimized structure b in HS state. On the other hand, crystallographic data reveal a C_2 symmetry for molecular structures at high temperature and no symmetry at low temperature. This disagreement is not totally unexpected because DFT methods give generally a lower symmetry for open shell molecular systems (i.e., HS states of Fe^{II}). Trying to optimize a molecule with "structure a" in the HS state with C_2 symmetry was not successful.

Finding multiple minima on the potential energy surface is often reported, particularly, in the case of different conformers of a molecule.[31] These studies can predict, for example, the conformational possibilities of a molecule with different geometries and energies and predicting the most stable conformer. In our case, with a large transition metal complex, this result might have been due to an artifact of the DFT calculation method. However, on one hand, the two optimized LS conformers reproduce fairly well the reported two X-ray crystallographic structures at low temperature (i.e., in the LS state). Especially, the distortion of the central atom group −N3−C10−C11−N4− is close to experimental ones. It is important to notice that this result has been obtained with all different computational methods (B3LYP, B3LYP*, HF, BP86, HCTH407). On the other hand, we should stress that the optimized LS and HS geometries (two minima, a global one and a local one in each spin state) should correspond to true minima because no imaginary vibrational frequencies were obtained in these cases. Furthermore, more accurate geometry optimizations have also been performed with tighter optimization convergence criteria (tightening the cutoffs on forces and step size for convergence), higher SCF (self-consistent field method) convergence criterion, and an ultrafine grid for integral calculations.[32] These tighter geometry optimizations confirmed also the existence of two conformers for which optimized structures correspond to two different "stationary points" on each minimum of the potential energy surface.

TABLE 4: Single-Point Electronic Energies of Each X-ray Molecular Structure Calculated (B3LYP*/TZVP) for Both Spin Multiplicities[a]

experimental structure	spin multiplicity	E (atomic units)	$\Delta E_{5,1}$ (kJ mol^{-1})
molecule Λ at 295 K	1	−2818.30928209	−72.1
	5	**−2818.33676310**	
molecule Δ at 295 K	1	−2818.30928183	−72.1
	5	**−2818.33676307**	
molecule Λ at 153 K	**1**	**−2818.27056146**	−70.7
	5	−2818.29747803	
molecule Δ at 153 K	1	−2818.26947025	−67.1
	5	**−2818.29504846**	
molecule Λ at 102 K	**1**	**−2818.18172226**	+12.9
	5	−2818.17681058	
molecule Δ at 102 K	**1**	**−2818.23907352**	+114.0
	5	−2818.19564392	

[a] Bold values correspond to the real spin multiplicities of the given structure.

Energies. First of all, electronic energies of each X-ray structures are discussed. After adding H atoms to the X-ray structures where it was missing and optimizing the H atom positions of each structure (freezing all the others atoms), single-point energies were calculated (Table 4). The values written in bold correspond to the real spin states of the molecule in the experiment at a given temperature. At 295 K, the two molecules are enantiomers, the slight difference in the energy values is negligible and occurs due to the experimental imprecision of atomic positions (and perhaps also to the theoretical addition of the H atoms). The calculated electronic energy of the molecules at 295 K indicates the stability of the HS state. This result is not surprising as single-point calculations have been performed for the two spin multiplicities on the same HS (!) X-ray crystallographic structure. At 153 K, the structures of the molecule Λ and Δ are slightly different, so the energy values are different too. The comparison between the spin states indicates that the HS state is more stable for both conformers. At 102 K, the Δ molecule is much more stable than the Λ molecule. Furthermore, at this temperature the LS form has a lower energy in agreement with the experimental facts. The important difference of the energy values between the molecules

TABLE 5: Electronic Energies Differences (ΔE, kJ mol^{-1}) Calculated by Different Functional Methods and Basis Sets

	B3LYP/ 6-31G*	B3LYP/ TZVP	B3LYP*/ 6-31G*	B3LYP*/ TZVP	HF/ TZVP	BP86/ TZVP	HCTH407/ TZVP
LSb-LSa	−11.7	−9.6	−12.5	−10.3	−1.52	−10.8	−14.6
HSa-LSa	−35.3	−40.9	−10.2	−16.4	−319	+59.2	−64.2
HSb-HSa	+5.6	+4.5	+4.6	+3.7	+9.3	+1.8	+0.3
HSb-LSb	−18.0	−26.8	+7.0	−2.3	−308.1	+71.9	−49.3

TABLE 6: Electronic Mean Polarizabilities[a] (Atomic Units) Calculated by Different Functional Methods and Basis Sets in Each Spin State and Conformer

	B3LYP/ 6-31G*	B3LYP*/ TZVP
α_{LS} (structure a)	353.27	390.90
α_{LS} (structure b)	350.39	388.68
α_{HS} (structure a)	342.87	379.18
α_{HS} (structure b)	346.07	382.93
$\Delta\alpha_{HL}$ (structure a)	−10.40	−11.72
$\Delta\alpha_{HL}$ (structure b)	−4.32	−5.75

[a] $\alpha = 1/3(\alpha_{xx} + \alpha_{yy} + \alpha_{zz})$.

Λ and Δ at 102 K compared to a slighter difference at 153 K, is consistent with the large conformational difference at 102 K.

On the other hand, electronic energies of the two optimized HS structures and the two LS ones are compared in Table 5 with different functional methods and basis sets. In the LS state, the optimized structure b has the lowest electronic energy, so it corresponds to the global minimum on the potential energy surface for the LS state. Indeed, this structure presents the smallest Fe−ligand bond lengths. Therefore the LS structure a corresponds to the local minimum. On the other hand, in the HS state the structure b has a slightly higher energy when compared to structure a.

The energy difference between the two LS state optimized conformational structures are around −12 kJ/mol (−1003 cm^{-1}) with all hybrid and GGA functional methods used, except for the HF methods with an small energy difference equal to −1.52 kJ/mol (−127.06 cm^{-1}) certainly due to the absence of dynamic electronic correlation in the calculation. As can be expected, HF methods highly overestimate the difference of the electronic energy between the LS and HS structures (ΔE_{HL}) with an energy much lower in the HS state. The BP86 method gives a ΔE_{HL} value, which is much higher than expected, but with the correct positive sign, the energy of the LS state being lower. In fact, it is the only method that gives the correct sign. It seems, however, that the reparametrized B3LYP* functional method, as compared to the B3LYP, gives a somewhat better result for ΔE_{HL}. Let us note here that the spin state electronic energies were often inaccurately calculated in the past.[26,27] Indeed, Reiher et al. suggested the B3LYP* functional, which is more accurate than B3LYP functional which often predicts wrong ground state multiplicity (HS state more stable). In their previous works on smaller complexes, Casida/Lawson Daku et al. thought that the B3LYP* and HTCH407 functional methods would correct this problem,[30] but it fails with our larger molecular complex and the spin state energy remains an unsolved problem.

Polarizability. The thermal variation of the dielectric constant at 100 kHz frequency for Fe[5-NO_2-sal-(1,4,7,10)] reveals the same transition temperatures and hysteresis and plateau widths as for the thermal variation of the magnetic susceptibility.[14] As mentioned before, the thermal variation of the dielectric constant of this compound is atypical as ϵ has a smaller value in the HS state ($\Delta\epsilon' = \epsilon'_{HS} - \epsilon'_{LS} = -0.13$). The change in dielectric constant of SCO materials results from both structural and electronic modifications accompanying the spin state change.[25] No relaxation process, associated with an orientational polarization of permanent dipole moments, is observed and the polarizability is therefore mainly composed of electronic and ionic contributions. As the HS molecules are more voluminous (due to the different occupation of antibonding e_g and nonbonding t_{2g} 3d orbitals of the central metal ion[1,2]) and the HS state has a more ionic nature, one would intuitively think that they have a higher polarizability. Indeed, for most of the investigated SCO compounds an increase of the macroscopically measurable ϵ' was observed during the LS to HS transition.[14] Therefore the negative value of $\Delta\epsilon'_{HL}$ observed in the compound Fe[5-NO_2-sal-(1,4,7,10)] can be considered as atypical.

Table 6 displays the calculated mean electronic polarizabilities in the two spin states for both conformers. We can see that the polarizabilities are slightly different between each conformer. More importantly, the calculated polarizability values are significantly higher in the LS states than in the HS state for both conformers. Though the relationship between the molecular polarizability (calculated in gas phase) and the macroscopic permittivity (measured in the solid state) is not straightforward in such a complex system, this result suggests that the experimentally observed variation of the dielectric constant upon the spin transition is principally due to the electronic polarization contribution. This result comes to complete our previous findings on a series of spin crossover complexes[25] and indicates that DFT calculations may predict the sign of $\Delta\epsilon$ in molecular spin crossover systems (at least for neutral complexes[28]). This initial approach points thus to the importance of structural considerations in the discussion of dielectric properties of SCO complexes but should, of course, be extended toward calculation methods taking into account the crystal lattice and not only a single molecule.

Conclusion

DFT calculations have been performed on the spin crossover complex Fe[5-NO_2-sal-(1,4,7,10)] starting from different X-ray crystallographic structures corresponding to the different stages of the two-step spin transition displayed by this material. Single-point energy studies of each X-ray structure and geometry optimizations have been performed followed by calculation of the electronic polarizabilities and vibrational frequencies. Two conformational isomers corresponding to a local and a global minima in the potential energy surface were found in both spin states. The structural differences between the two calculated conformers are in good agreement with the experimental observations. This finding confirms thus the X-ray crystallographic results of Boinnard et al.,[4] which were questioned in later reports.[13] Furthermore, it shows also the potential of DFT calculations in predicting the existence of conformers in large transition metal complexes and even their relative stability. On the other hand, the energy gap between the two forms with different spin multiplicities cannot be reliably determined at this level of the DFT. Finally, the calculated electronic polarizabilities comfort further the hypothesis about the origin of the dielectric constant change accompanying the spin transition.

Acknowledgment. DFT calculations have been performed thanks to the facilities provided by CALMIP (Calculs en Midi-

Pyrénées, France), CINES (Centre Informatique National de l'Enseignement Supérieur, France), and IDRIS (Institut du Développement et des Ressources en Informatique Scientifique).

Supporting Information Available: Bond lengths and angles calculated using the different DFT functionals and bases. This material is available free of charge via the Internet at http://pubs.acs.org.

References and Notes

(1) Gütlich, P.; Hauser, A.; Spiering, H. *Angew. Chem., Int. Ed. Engl.* **1994**, *33*, 2024.

(2) Spin Crossover in Transition Metal Compounds I−III. In *Topics in Current Chemistry*; Gütlich, P., Goodwin, H.A., Eds.; Springer: Berlin, 2004; Vols. 233−235.

(3) Petrouleas, V.; Tuchagues, J.-P. *Chem. Phys. Lett.* **1987**, *137*, 21.

(4) Boinnard, D.; Bousseksou, A.; Dworkin, A.; Savariault, J.-M.; Varret, F.; Tuchagues, J.-P. *Inorg. Chem.* **1994**, *33*, 271.

(5) Köppen, H.; Müller, E. W.; Köhler, C. P.; Spiering, H.; Meissner, E.; Gütlich, P. *Chem. Phys. Lett.* **1982**, *91*, 348.

(6) Real, J. A.; Bolvin, H.; Bousseksou, A.; Dworkin, A.; Kahn, O.; Varret, F.; Zarembowitch, J. *J. Am. Chem. Soc.* **1992**, *114*, 4650.

(7) Chernyshov, D.; Hostettler, M.; Törnroos, K. W.; Bürgi, H.-B. *Angew. Chem., Int. Ed.* **2003**, *42*, 3825.

(8) Bousseksou, A.; Nasser, J.; Linares, J.; Boukheddaden, K.; Varret, F. *J. Phys. I Fr.* **1992**, *23*, 1381.

(9) Jacobi, R.; Spiering, H.; Gütlich, P. *J. Phys. Chem. Solids* **1992**, *53*, 267.

(10) Bousseksou, A.; Varret, F.; Nasser, J. *J. Phys. I Fr.* **1993**, *3*, 1463.

(11) Boukheddaden, K.; Linares, J.; Codjovi, E.; Varret, F.; Niel, V.; Real, J. A. *J. Appl. Phys.* **2003**, *93*, 7103.

(12) Zein, S.; Borshch, S. A. *J. Am. Chem. Soc.* **2005**, *127*, 16197.

(13) (a) Salmon, L.; Bousseksou, A.; Donnadieu, B.; Tuchagues, J.-P. *Inorg. Chem.* **2005**, *44*, 1763. (b) Salmon, L. Ph.D. Thesis, University of Paul Sabatier, Toulouse, France, 1999.

(14) Bousseksou, A.; Molnár, G.; Demont, P.; Menegotto, J. *J. Mater. Chem.* **2003**, *13*, 2069.

(15) Frisch, M. J.; et al. *Gaussian 03*, revision B.05; Gaussian, Inc.: Pittsburgh, PA, 2003.

(16) (a) Becke, A. D. *J. Chem. Phys.* **1993**, *98*, 5648. (b) *Becke3LYP Method References and General Citation Guidelines, Gaussian News*, **1994**, *5*, 2.

(17) Reiher, M. *Inorg. Chem.* **2002**, *41*, 6928.

(18) Schäfer, A.; Huber, C.; Ahlrichs, R. *J. Chem. Phys.* **1994**, *100*, 5829.

(19) (a) Dunning, T. H., Jr.; Hay, P. J. In *Modern Theoretical Chemistry*; Schaefer, H. F., III, Ed.; Plenum: New York, 1976; Vol. 3, pp 1−28. (b) Hay, P. J.; Wadt, W. R. *J. Chem. Phys.* **1985**, *82*, 270.

(20) http://www.accelrys.com/products/mstudio/.

(21) http://www.accelrys.com/products/cerius2/refs.html.

(22) http://www.accelrys.com/products/insight/references.html.

(23) Schaftenaar, G.; Noordik, J. H. MOLDEN 4.4 *J. Comput.-Aided Mol. Design* **2000**, *14*, 123.

(24) (a) Flükiger, P.; Lüthi, H. P.; Portmann, S.; Weber, J. MOLEKEL 4.3; Swiss Center for Scientific Computing, Manno, Switzerland, 2000−2002. (b) Portmann, S.; Lüthi, H. P. *Chimia* **2000**, *54*, 766.

(25) Bonhommeau, S.; Guillon, T.; Lawson Daku, L. M.; Demont, P.; Sanchez Costa, J.; Létard, J.-F.; Molnár, G.; Bousseksou, A. *Angew. Chem. Int. Ed.* **2006**, *45*, 1625.

(26) (a) Paulsen, H.; Trautwein, A. X. *Top. Curr. Chem.* **2004**, *235*, 197. (b) Paulsen, H.; Duelund, L.; Winkler, H.; Toftlund, H.; Trautwein, A. X. *Inorg. Chem.* **2001**, *40*, 2201.

(27) (a) Reiher, M.; Salomon, O.; Hess, B. A. *Theor. Chem. Acc.* **2001**, *107*, 48. (b) Salomon, O.; Reiher, M.; Hess, B. A. *J. Chem. Phys.* **2002**, *117*, 4729.

(28) Guillon, T.; Bonhommeau, S.; Sanchez Costa, J.; Zwick, A.; Létard, J.-F.; Demont, P.; Molnár, G.; Bousseksou, A. *Phys. Stat. Solidi (a)* **2006**, *11*, 2974.

(29) (a) Baranovic, G. *Chem. Phys. Lett.* **2003**, *369*, 668. (b) Brehm, G.; Reiher, M.; Schneider, S. *J. Phys. Chem. A* **2002**, *106*, 12024. (c) Pálfi, V. K.; Guillon, T.; Paulsen, H.; Molnár, G.; Bousseksou, A. *C.R. Chimie* **2005**, *8*, 1317. (d) Paulsen, H.; Trautwein, A. X. *J. Phys. Chem. Solids* **2004**, *65*, 793. (e) Paulsen, H.; Winkler, H.; Trautwein, A. X.; Grunsteudel, H.; Rusanov, V.; Toftlund, H. *Phys. Rev. B* **1999**, *59*, 975. (f) Reiher, M. *Inorg. Chem.* **2002**, *41*, 6928. (g) Zein, S.; Matouzenko, G. S.; Borshch, S. A. *Chem. Phys. Lett.* **2004**, *397*, 475. (h) Zein, S.; Matouzenko, G. S.; Borshch, S. A. *J. Phys. Chem. A* **2005**, *109*, 8568.

(30) (a) Fouqueau, A.; Mer, S.; Casida, M. E.; Lawson Daku, L. M.; Hauser, A.; Mineva, T.; Neese, F. *J. Chem. Phys.* **2004**, *120*, 9473. (b) Fouqueau, A.; Casida, M. E.; Lawson Daku, L. M.; Hauser, A.; Neese, F. *J. Chem. Phys.* **2005**, *122*, 044110. (c) Lawson Daku, L. M.; Vargas, A.; Hauser, A.; Fouqueau, A.; Casida, M. E. *ChemPhysChem* **2005**, *6*, 1393.

(31) http://www.gaussian.com/g_ur/g03mantop.htm.

(32) (a) Ciofini, I.; Daul, C. A.; Adamo, C. *J. Phys. Chem. A* **2003**, *107*, 11182. (b) Zheng, X.; Wang, B.; Englert, U.; Herberich, G. E. *Inorg. Chem.* **2001**, *40*, 3117. (c) Catellani, M.; Mealli, C.; Motti, E.; Paoli, P.; Perez-Carren, E.; Pregosin, P. S. *J. Am. Chem. Soc.* **2002**, *124*, 4336. (d) Jensen, V. R.; Koley, D.; Jagadeesh, M. N.; Thiel, W. *Macromolecules* **2005**, *38*, 10266. (e) Veiros, L. F. *Chem. Eur. J.* **2005**, *11*, 2505. (f) Suwattanamala, A.; Magalhães, A. L.; Gomes, J. A. N. F. *Chem. Phys.* **2005**, *310*, 109. (g) Grummt, U.-W.; Erhardt, S. *J. Mol. Struct.* (*THEOCHEM*) **2004**, *685*, 133.